metals

Article

Transient Effects in Creep of Sanicro 25 Austenitic Steel and Their Modelling

Luboš Kloc [1,*], Václav Sklenička [1,2] and Petr Dymáček [1,2]

1 Institute of Physics of Materials AS CR, v.v.i. Žižkova 22, CZ-61662 Brno, Czech Republic; vsklen@ipm.cz (V.S.); pdymacek@ipm.cz (P.D.)
2 CEITEC IPM, Institute of Physics of Materials AS CR, v.v.i. Žižkova 22, CZ-61662 Brno, Czech Republic
* Correspondence: kloc@ipm.cz

Received: 15 January 2019; Accepted: 15 February 2019; Published: 19 February 2019

Abstract: Transient effects upon stress changes during creep of the new Sanicro 25 steel were investigated experimentally using the helicoid spring specimen technique. The creep behaviour was found to be qualitatively the same as that observed earlier with the creep-resistant 9% Cr ferritic-martensitic P-91 steel, but the transient strains are considerably smaller. Negative creep rate, which is strain running against the applied stress, was observed with any stress decrease. Parameters for the complex creep model were estimated and model results were compared to the creep rates measured experimentally. The model can be used for the finite element method modelling of the creep and stress relaxation effects in the components made from the Sanicro 25 steel.

Keywords: creep; transient effects; Sanicro 25; high temperature steels

1. Introduction

New materials capable of withstanding loading at high temperatures for long periods of time are demanded and have been developed in order to improve efficiency of the thermal power plants. The austenitic stainless steel Sandvik Sanicro 25 (UNS S31035) steel was recently developed within the Termie–AD 700 project in Europe and as a prospective material has been subjected to various mechanical testing [1–4].

Austenitic steels exhibit better creep and corrosion resistance than ferritic ones, but, due to lower thermal conductivity and higher thermal expansion, are sensitive to thermomechanical fatigue. The finite element method (FEM) is an apt tool to describe the behaviour of real components under transient conditions. A relevant mathematical description of the material's properties under a wide range of stresses and temperatures is needed to obtain valid results. The current descriptions of the creep processes are based exclusively on the creep curves measured under constant loading conditions, so the transient effects caused by stress changes are ignored. This approach is unsatisfactory [5].

Since the demanded creep lives are obviously very long, creep tests under conditions close to that used in industrial application of the material cannot be done. Extrapolation from the results of the tests accelerated by higher temperature and/or stress is used instead. An alternative approach is measurement of very small creep strains, revealing the creep behaviour at the very beginning of the creep curve. This approach is very rare [6,7], though the results are important for parts with very small tolerable strains and mainly for relaxation of stresses generated for instance by temperature gradients. The results obtained for the creep resistant steels [8] show that the extrapolation method mentioned above does not provide correct description of the small creep strains. The measurement of the small creep strains was used in this work to obtain a basis for the realistic FEM modelling of the thermomechanical fatigue of the prospective Sanicro 25 steel.

In this work, transient strains during creep of the Sanicro 25 steel are investigated under conditions close to the potential service employment of the steel. A helicoid spring specimen technique was used to get high strain sensitivity. The main aim of the work is to explore transient effects in creep of the prospective Sanicro 25 steel, and, together with our previous paper [9], to collect data for the complex phenomenological creep model [10], the only model capable of describing transient effects in creep. While the previous paper [9] was devoted to constant stress tests, this work is focused on the transient stages upon stress changes.

2. Experimental Material and Procedure

2.1. Material

Material for experiments was supplied by Sandvik Materials Technology, Sandviken, Sweden in the form of a cylindrical rod of 150 mm in diameter. Chemical composition of the material is listed in Table 1.

Table 1. Chemical composition of tested material (in wt.%).

C	Si	Mn	Cr	Ni	W	Co	Cu	Nb	N	Fe
0.1	0.2	0.5	22.5	25.0	3.6	1.5	3.0	0.5	0.23	Bal.

Specimens were tested in the as-received state of the material. The microstructure of the material was briefly described in our previous paper [9]. Grain size is generally of about 25 µm, but grains as large as 200 µm can be also observed. Grain boundaries are decorated by small Nb rich carbonitrides and some such particles occur also in the grain interiors, mainly in large grains. Microstructure of the material has been analysed in detail in previously published papers [11–14] and is not studied here, since the very small creep strains do not cause visible changes in the microstructure.

2.2. Creep Tests

The helicoid spring specimen technique were used to investigate creep responses on the stress changes at temperatures 700 and 750 °C and stresses between 25 and 90 MPa. The technique enables measurement of very small creep strains and then also very low creep rates within tests of acceptable duration. The experimental arrangement was described in detail in [15].

The shape and manufacturing process of the specimens were the same as in the previous work [9]. Special processing technology combining precision conventional machining and electroerosive cutting was used to manufacture helicoid spring specimens with an outer diameter of 34 mm, an inner diameter of 31 mm, a pitch of 3 mm and an overall length of 50 mm. The procedure was optimised to minimise any influence on the microstructure of the specimen. The creep tests were conducted in a protective atmosphere of purified argon. Testing temperature was kept within the ±1 °C interval and the homogeneity of the temperature field was in the same order. The contactless optical measurement of strain was used to avoid any friction or other disturbing factors.

3. Results

3.1. Creep Curves

Measured creep curves are shown in Figures 1 and 2. Clear transient stages are observed following all stress changes. The transient strains are not so extensive as those observed with the 9% Cr ferritic-martensitic P-91 steel [16] but are still important.

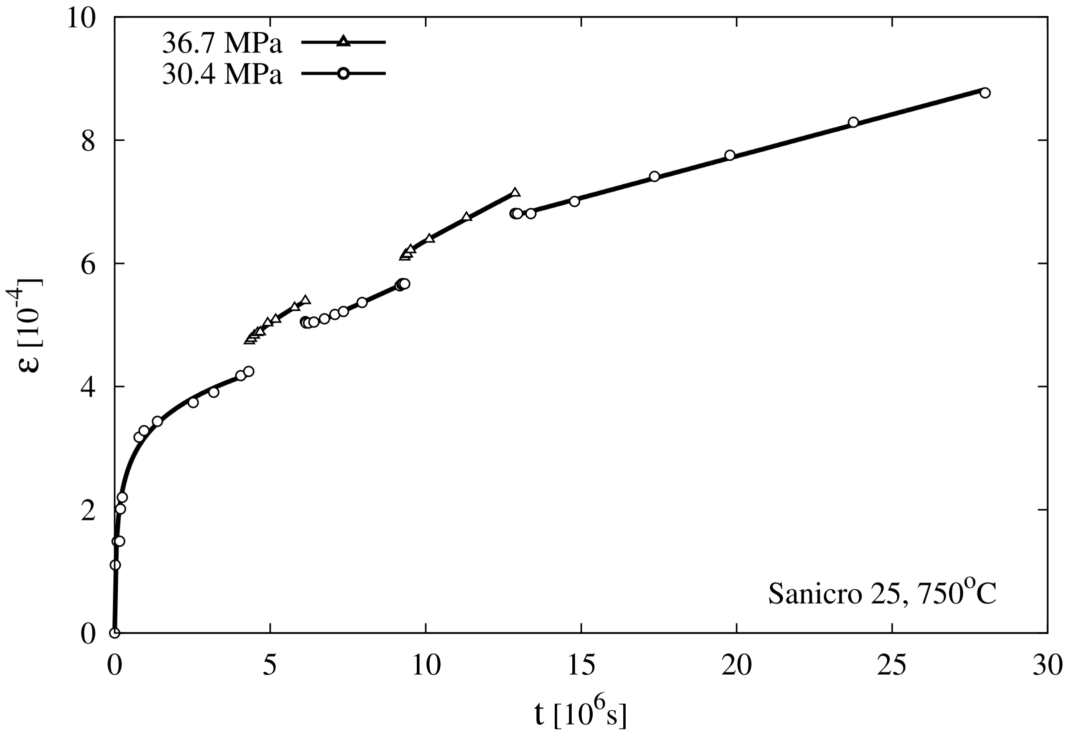

Figure 1. Creep curves at 750 °C and stresses 30.4 and 36.7 MPa. Experimental data (points) were fitted by Li equation [17] (lines).

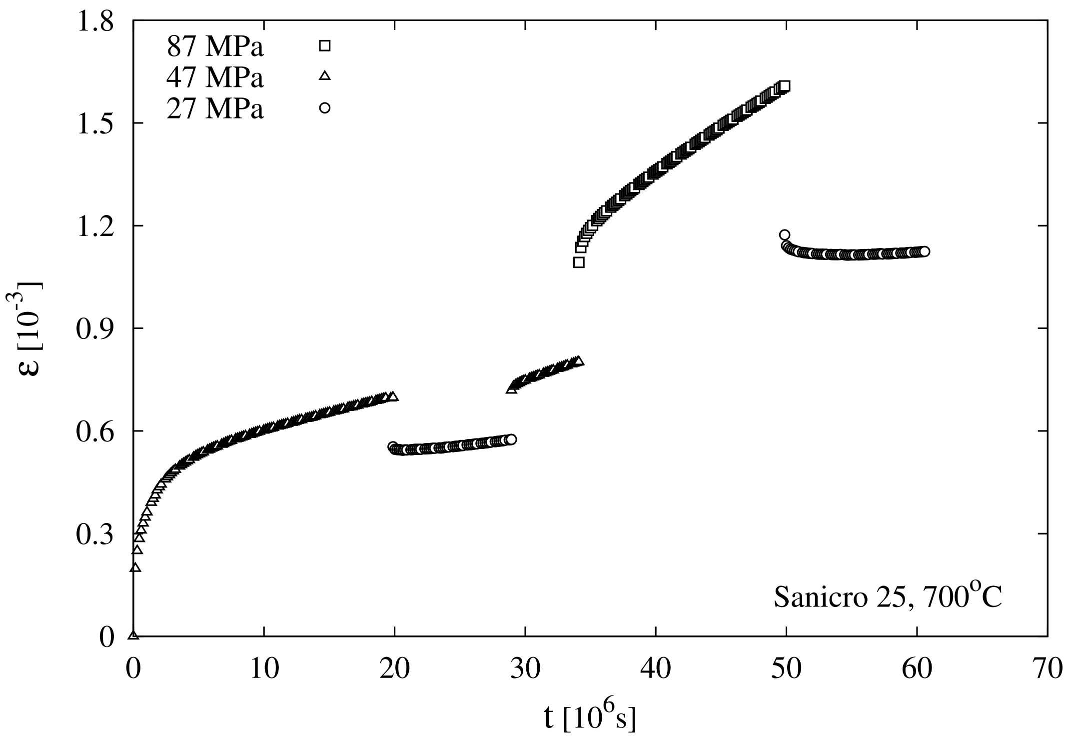

Figure 2. Creep curves at 700 °C and stresses from 27 to 87 MPa.

The short period of negative strain rate, which is strain running against applied stress, is observable even at relatively small stress reductions, indicating importance of internal stresses. This effect is visible on the creep curve detail in Figure 3.

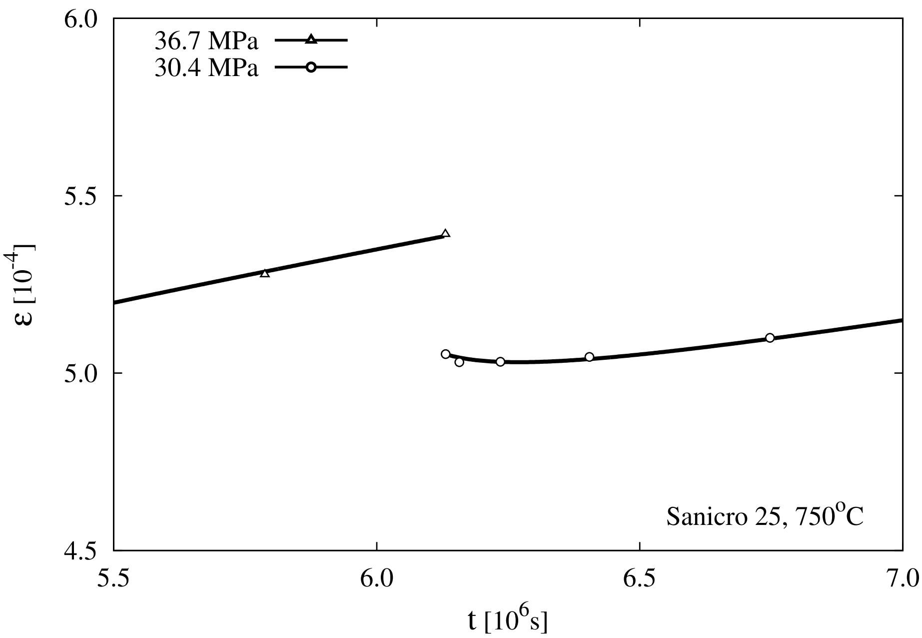

Figure 3. Detail of the creep curve at 750 °C and stress reduction from 36.7 to 30.4 MPa.

The data required to reproduce these findings are available to download from http://dx.doi.org/10.17632/bjw2mtgswp.1#file-a218d703-a6a8-49f7-b765-2080252c050a.

3.2. Creep Rates

Creep rates measured at the end of each segment of the creep curve are plotted in Figure 4 together with the results of constant stress tests from [9]. It is clear that, for the low-stress creep mechanism, there is no steady state creep stage, but strain rate is permanently decreasing. This is the same behaviour as it was observed with the P-91 steel [16].

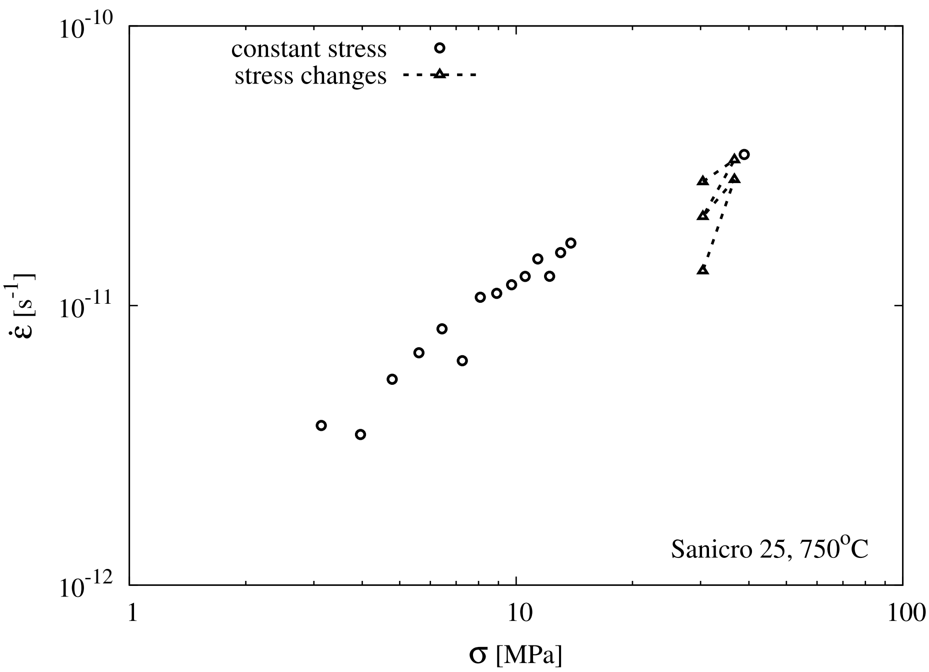

Figure 4. The creep rates $\dot{\varepsilon}$ for 750 °C, measured at the end of each creep curve segment. The creep rates from constant stress tests [9] are plotted for comparison.

4. Model

4.1. Creep Rate Description

A complex phenomenological model [10] can be used to describe observed transient effects. The model is based on an assumption of two independent deformation mechanisms, acting in parallel. The first mechanism, dominating at low stresses, is anelastic and its principle is a building of the field of internal stresses, assuming interaction of the hard elastic zones and soft elastoplastic zones. The other mechanism, dominating at higher stresses, is more obvious plastic deformation described by the modified Garofallo equation with threshold stress.

Overall creep rate $\dot{\varepsilon}$ is expressed by modified Li equation as

$$\dot{\varepsilon} = \frac{\dot{\sigma}}{E} + \dot{\varepsilon}_c + \frac{\dot{\varepsilon}_s \left(1 + r_i\right)}{1 + r_i - r_i \exp\left(-\theta\right)}, \tag{1}$$

where $\dot{\varepsilon}_s$ is given by

$$\dot{\varepsilon}_s = \operatorname{sgn}(\sigma)\, b \exp\left(\frac{-Q_h}{RT}\right) \sinh\left(p\left(|\sigma| + \sqrt{\left(|\sigma| - \sigma_t\right)^2 + \sigma_r^2} - \sqrt{\sigma_t^2 + \sigma_r^2}\right)\right), \tag{2}$$

the "creep age" θ is integrated according to

$$\theta = \frac{1}{c}\int_0^t |\dot{\varepsilon}_s| \,\mathrm{d}t, \tag{3}$$

and $\dot{\varepsilon}_c$ is obtained by the numerical solution of the equation

$$\dot{\varepsilon}_c = g \exp\left(\frac{-Q_l}{RT}\right)\left(\frac{\sigma}{\sigma_t} - \frac{(1-k)E}{k\sigma_t}\varepsilon_c\right)^3. \tag{4}$$

In the above equations, σ is the applied stress, T is absolute temperature, and Q_h and Q_l are the apparent activation energies for the high-stress and low-stress mechanisms, respectively, E is Young's modulus, σ_t is threshold stress, σ_r, describes the residual effective stress below the threshold, r_i describes the ratio between initial and secondary creep rate, b controls the overall rate of the high-stress mechanism, p controls the transition between linear and exponential parts of the Garofallo equation, c describes the relation between the secondary stage creep rate and the primary relaxation time of the high-stress mechanism, g controls the overall rate of the low-stress mechanism and k describes the ratio between hard and soft zones.

4.2. Model Results

The parameter values used to model the creep behaviour of the Sanicro 25 steel are summarised in Table 2. The temperature dependence of the parameter σ_r must be introduced to obtain acceptable results, but with experiments at only two temperature levels, it is not possible to speculate about the character of that dependence.

Table 2. Set of model parameters for the Sanicro 25 steel.

Parameter	Value	Unit	
σ_t	130	MPa	
σ_r	3.0	MPa	@700 °C
σ_r	1.0	MPa	@750 °C
r_i	8.0		
b	3.0×10^{19}	s^{-1}	
p	0.03	MPa^{-1}	
Q_h	525	kJ/mol	
Q_l	171	kJ/mol	
g	700	s^{-1}	
E	139×10^3	MPa	
k	0.65		
c	3.5×10^{-3}		

Model results for the constant-stress creep experiments from [9] and [18] are showed in Figures 5–7, exhibiting good results for both low-stress and high-stress creep regimes.

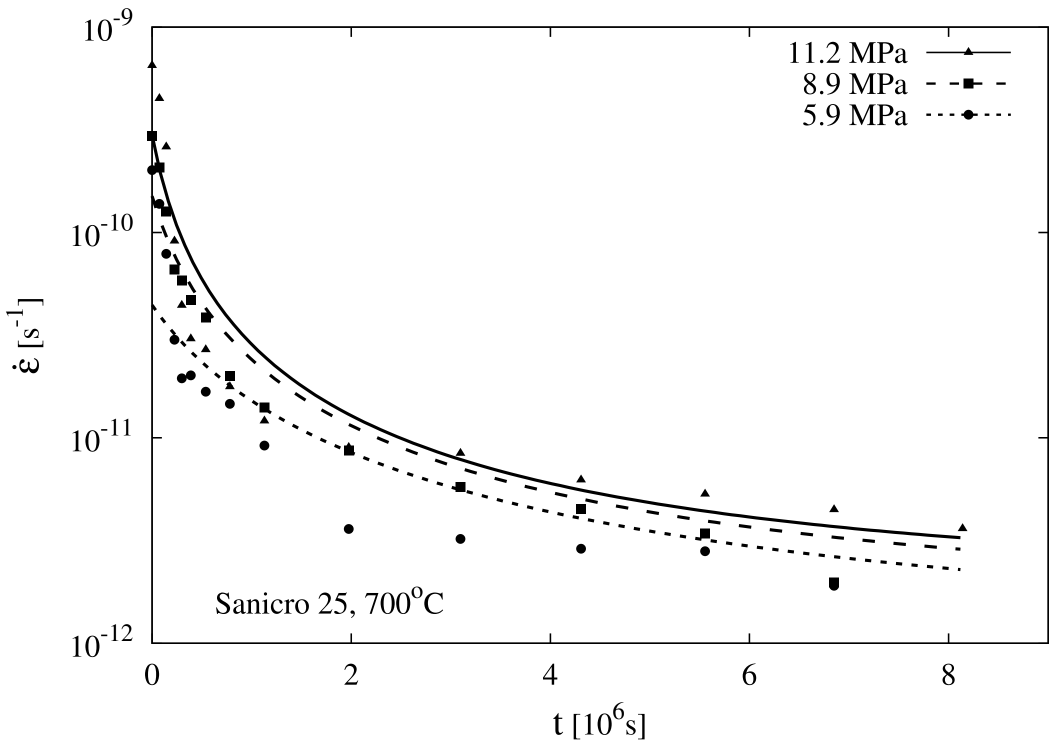

Figure 5. Creep rate dependence on time for Sanicro 25 at 700 °C and low stresses [9] (points) compared to model results (lines).

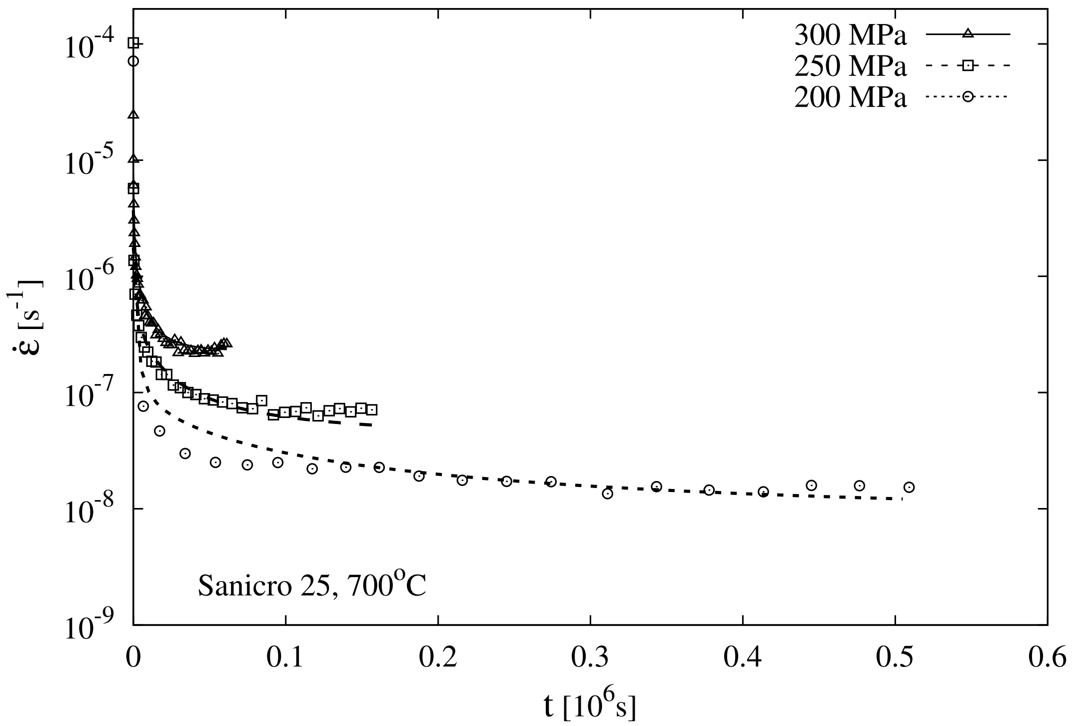

Figure 6. Creep rate dependence on time for Sanicro 25 at 700 °C and high stresses [18] (points) compared to model results (lines).

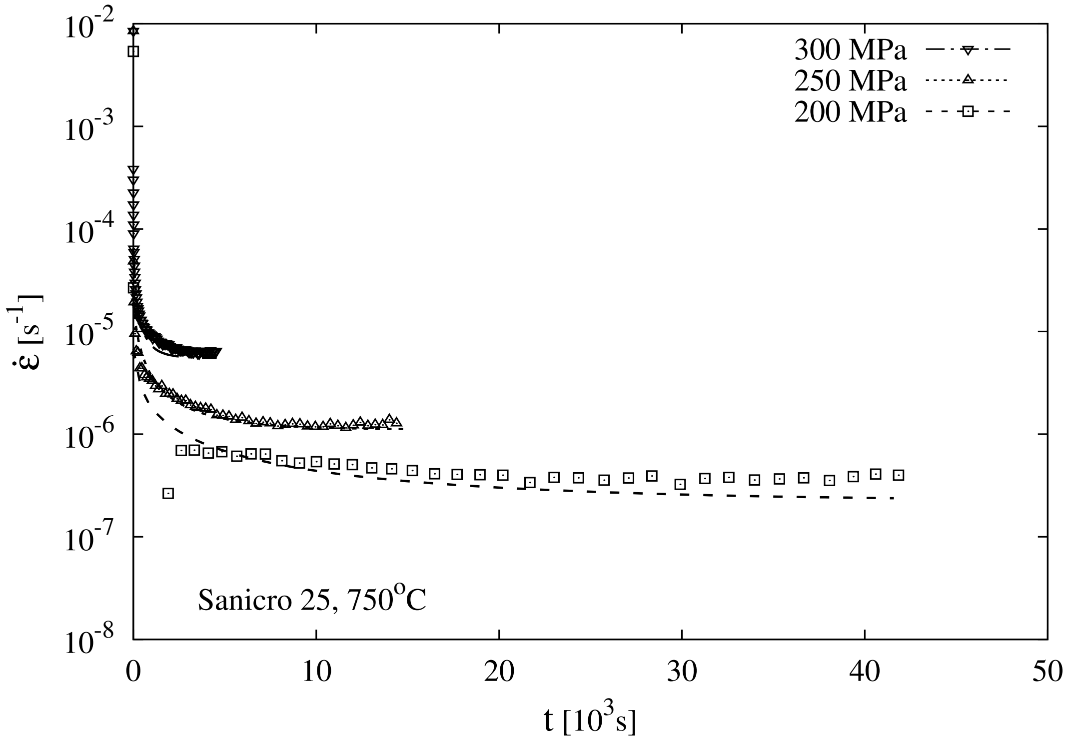

Figure 7. Creep rate dependence on time for Sanicro 25 at 750 °C and high stresses [18] (points) compared to model results (lines).

Model results for the above presented creep experiments with stress changes are plotted in Figures 8 and 9.

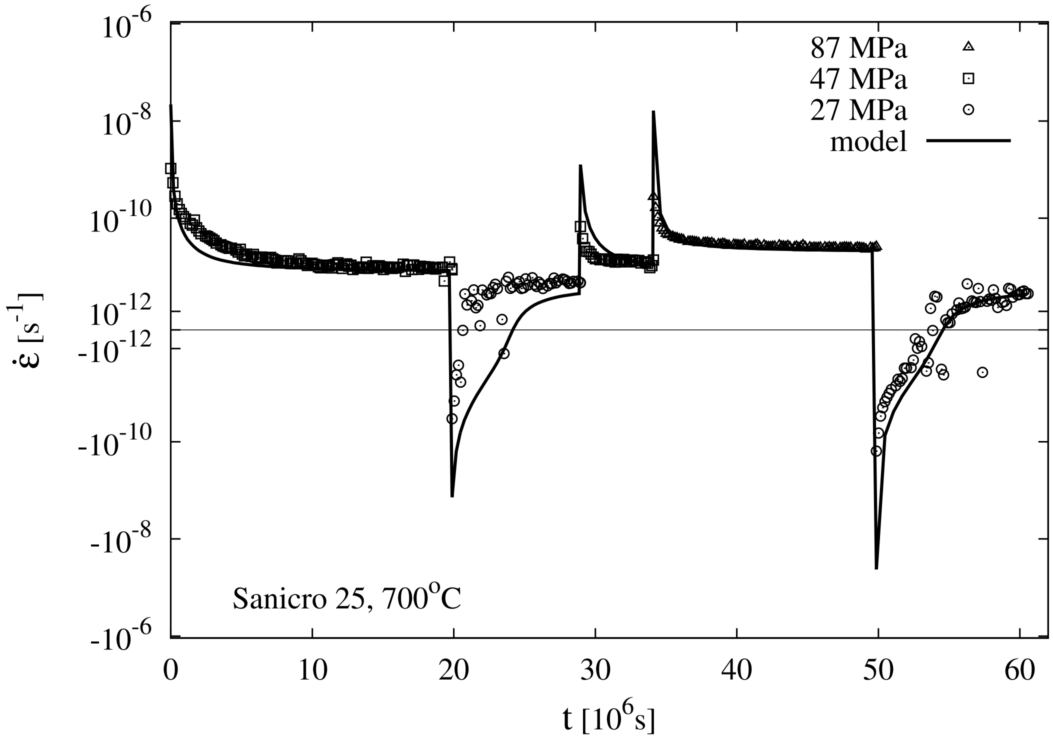

Figure 8. Creep rate dependence on time for Sanicro 25 at 700 °C and stress changes (points) compared to model results (line).

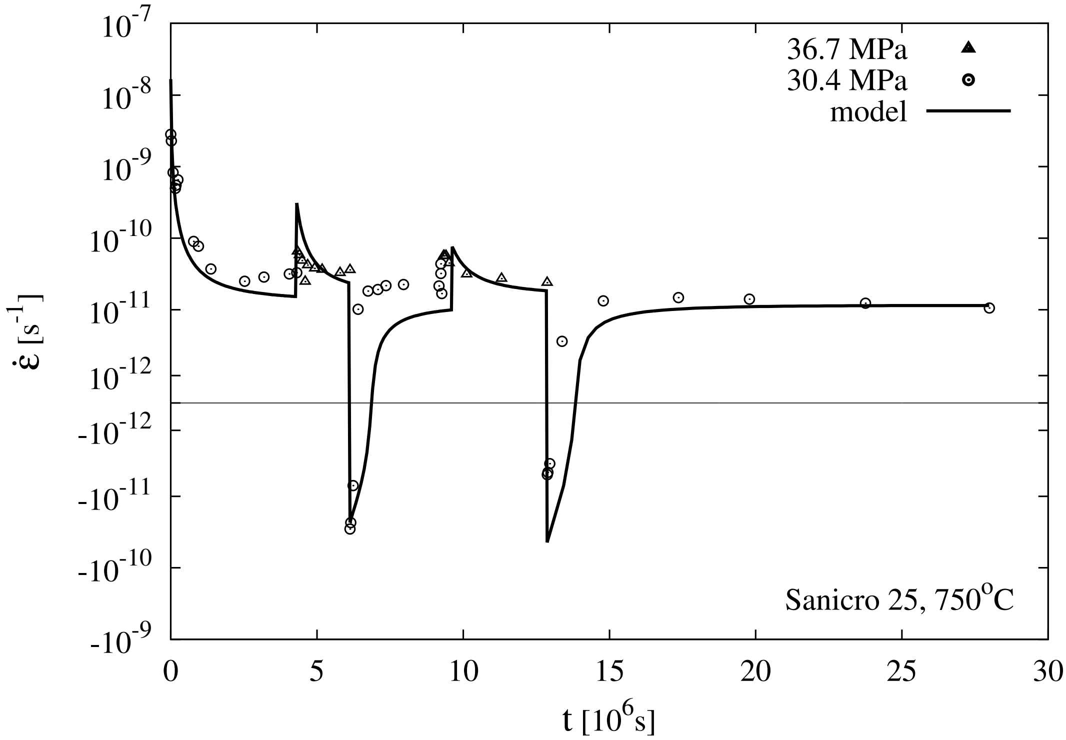

Figure 9. Creep rate dependence on time for Sanicro 25 at 750 °C and stress changes (points) compared to model results (line).

4.3. Discussion

The results are not perfect, mainly during early stress decreases and around zero strain rates. The time duration of the transient stage is slightly overestimated in the model. Some creep curves or segments of the creep curves with stress changes are fitted well, while with others the fit is considerably worse. There are two reasons for that effect. First, there is some natural scatter in the experimentally observed values. As was pointed out in the previous paper [9], the scatter in the initial creep rates is considerably higher than that of the creep rate in a secondary stage. Thus, the shape of creep curves varies and it is not possible to describe them by one set of parameters. Compromise values were then adopted for parameters r_i and k, satisfying some creep curves better than others. Second, the model was derived using many strong assumptions, which are not necessarily strictly fulfilled. All these assumptions are listed in [10]. Probably, the two deformation mechanisms are not completely independent. This fact can explain some systematic deviations of the model predictions from the experimental curves. Taking into account that other creep models ignore the transient effects completely, it can be considered as acceptable.

5. Conclusions

The transient creep behaviour upon the stress changes of the Sanicro 25 austenitic creep resistant steel was investigated at temperatures 700 and 750 °C and the applied stresses between 25 and 90 MPa.

The strain reactions to the stress changes are qualitatively the same as those observed for the P-91 ferritic steel [16], but the transient strains are considerably smaller. In the low-stress creep regime, time period of the negative creep rate is observed even with relatively small decreases in the applied stress.

The complex phenomenological creep model published in [10] was used to describe primary and secondary stages of the creep behaviour of the Sanicro 25 steel under various conditions including transient effects. All parameters of the model were estimated and the model can be used in FEM calculations, though the results are not perfect.

Author Contributions: Conceptualization, L.K.; methodology, L.K.; validation, V.S. and L.K.; investigation, L.K. and P.D.; resources, P.D. and L.K.; data curation, P.D.; writing–original draft preparation, L.K.; writing–review and editing, V.S. and P.D.; visualisation, L.K.; supervision, V.S.; project administration, L.K.; funding acquisition, L.K.

Funding: This research was funded by the Czech Science Foundation under contract no. 15-21394S and partly accomplished in CEITEC 2020 (LQ1601) with financial support from the Ministry of Education, Youth and Sports of the Czech Republic under the National Sustainability Programme II.

Acknowledgments: The authors want to thank Guocai Chai from Sandvik Materials Technology for the supply of the Sanicro 25 experimental material.

Conflicts of Interest: The authors declare no conflict of interest.

Abbreviations

The following abbreviations are used in this manuscript:

FEM Finite Element Method

References

1. Chai, G.; Bostrom, M.; Olaison, M.; Forsberg, U. Creep and LCF Behaviors of Newly Developed Advanced Heat Resistant Austenitic Stainless Steel for A-USC. *Procedia Eng.* **2013**, *55*, 232–239. [CrossRef]
2. Polak, J.; Petras, R.; Heczko, M.; Kruml, T.; Chai, G. Evolution of the cyclic plastic response of Sanicro 25 steel cycled at ambient and elevated temperatures. *Int. J. Fatigue* **2016**, *83*, 75–83. [CrossRef]
3. Petras, R.; Skorik, V.; Polak, J. Thermomechanical fatigue and damage mechanisms in Sanicro 25 steel. *Mater. Sci. Eng. A* **2016**, *650*, 52–62. [CrossRef]

4. Chai, G.; Forsberg, U. Sanicro 25: An advanced high-strength, heat-resistant austenitic stainless steel. In *Materials for Ultra-Supercritical and Advanced Ultra-Supercritical Power Plants*; DiGianfrancesco, A., Ed.; Number 104 in Series in Energy; Woodhead Publishing: Cambridge, UK: 2017; pp. 391–421.
5. Kloc, L. Critical View on the Creep Modelling Procedures. *Acta Phys. Pol. A* **2015**, *128*, 540–542. [CrossRef]
6. Sritharan, T.; Jones, H. Creep of Type-316 Stainless-steel at Low Stresses. *Met. Sci.* **1989**, *15*, 365–368. [CrossRef]
7. Mishra, R.S.; Jones, H.; Greenwood, G.W. Creep of a low carbon steel at low stresses and intermediate temperatures. *Acta Metall. Mater.* **1990**, *38*, 461–468. [CrossRef]
8. Kloc, L.; Skienicka, V.; Ventruba, J. Comparison of low stress creep properties of ferritic and austenitic creep resistant steels. *Mater. Sci. Eng. A* **2001**, *319*, 774–778. [CrossRef]
9. Kloc, L.; Dymáček, P.; Sklenička, V. High temperature creep of Sanicro 25 austenitic steel at low stresses. *Mater. Sci. Eng. A* **2018**, *722*, 88–92. [CrossRef]
10. Kloc, L.; Sklenička, V.; Dymáček, P.; Plešek, J. New creep constitutive equation for finite element modelling including transient effects. *Mech. Mater.* **2018**, *119*, 49–55. [CrossRef]
11. Heczko, M.; Polak, J.; Kruml, T. Microstructure and dislocation arrangements in Sanicro 25 steel fatigued at ambient and elevated temperatures. *Mater. Sci. Eng. A* **2017**, *680*, 168–181. [CrossRef]
12. Polak, J.; Petras, R.; Heczko, M.; Kubena, I.; Kruml, T.; Chai, G.C. Low cycle fatigue behavior of Sanicro 25 steel at room and at elevated temperature. *Mater. Sci. Eng. A* **2014**, *615*, 175–182. [CrossRef]
13. Zhou, R.Y.; Zhu, L.H.; Liu, Y.Y.; Lu, Z.R.; Chen, L.; Ma, X. Microstructural evolution and the effect on hardness of Sanicro 25 welded joint base metal after creep at 973 K. *J. Mater. Sci.* **2017**, *52*, 6161–6172. [CrossRef]
14. Calmunger, M.; Chai, G.C.; Eriksson, R.; Johansson, S.; Moverare, J.J. Characterization of Austenitic Stainless Steels Deformed at Elevated Temperature. *Metall. Mater. Trans. A-Phys. Metall. Mater. Sci.* **2017**, *48A*, 4525–4538. [CrossRef]
15. Kloc, L.; Marecek, P. Measurement of Very Low Creep Strains: A Review. *J. Test. Eval.* **2009**, *37*, 53–58.
16. Kloc, L.; Sklenicka, V. Confirmation of low stress creep regime in 9% chromium steel by stress change creep experiments. *Mater. Sci. Eng. A* **2004**, *387*, 633–638. [CrossRef]
17. Li, J. A Dislocation Mechanism of Transient Creep. *Acta Metall.* **1963**, *11*, 1269–1270. [CrossRef]
18. Dymacek, P.; Dobes, F.; Kloc, L. Small Punch Testing of Sanicro 25 Steel and its Correlation with Uniaxial Tests. *Key Eng. Mater.* **2017**, *734*, 70–76. [CrossRef]